

## Corrosion Inhibitor Film Forming in Aerated and Deaerated Solutions

Ahmed Y. Musa\*, Abdul Amir H. Kadhum, Abu Baker Muhamad

Department of Chemical and Process Engineering, Faculty of Engineering and Built Environment, Universiti Kebangsaan Malaysia, Bangi, 43600, Selangor, Malaysia.

\*E-mail: [ahmed.musa@ymail.com](mailto:ahmed.musa@ymail.com), [ahmedym@vlsi.eng.ukm.my](mailto:ahmedym@vlsi.eng.ukm.my)

Received: 2 September 2010 / Accepted: 15 September 2010 / Published: 1 December 2010

---

The behavior of corrosion inhibitor (4-amino-5-phenyl-4H-1, 2, 4-triazole-3-thiol (APTT)) film under turbulent flow condition in oxygenated and de aerated solutions was studied. Turbulent flow condition experiments were simulated by rotating cylinder electrode (RCE). Change of open circuit potential (OCP) with immersion time, Direct-current (potentiodynamic polarization) and alternating-current (electrochemical impedance spectroscopy (EIS)) were used to study the effect of turbulent flow on the formation of inhibitor film. OCP was observed to shift toward positive values in oxygenated solution and shifted toward negative values in de aerated solution with rotation rate. Inhibition efficiencies were decreased with rotation rate in oxygenated solution, while it kept almost constant in de aerated solution. Results obtained from changes of open circuit potential (OCP) with immersion time, potentiodynamic polarization, and impedance measurements are in good agreement and indicated that the formation and the development of the inhibitor film were flow rate dependant.

---

**Keywords:** Corrosion, turbulent flow, inhibitor film, APTT.

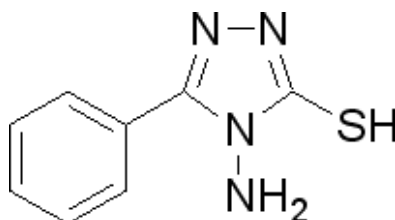
### 1. INTRODUCTION

In the industry related to mechanical machining, cutting tools and cooling systems are often subjected to aggressive conditions (turbulent flow, high temperature, etc.), involving the early apparition of corrosion. The addition of inhibitors in lubricating or rinsing solutions presents nowadays good results to prevent corrosion, and then prolong system lifetime [1].

There have been few systematic studies reporting the effect of flow on the metals corrosion which have carefully controlled the flow parameters [2-4]. Ochoa et al. [5] have studied the behavior of the interface carbon steel in 200mg l<sup>-1</sup> NaCl solution with inhibitor (fatty amines associated with phos-phono-carboxylic acid salts) using a rotating disk electrode. They have pointed out that the

properties of the protective layer were dependent on the electrode rotation rate where current densities decrease when the electrode rotation rate increases. Mora-Mendoza et al. [6] have studied the corrosion inhibition of mild steel under turbulent flow conditions; he has demonstrated that the localized corrosion process does not occur at a specific rotation speed and they have shown that the changes in  $E_{corr}$  to more positive values are more important in producing the localized process and removing the electrostatically adsorbed inhibitor from the surface sample, than increases in shear stress that generated from the turbulent flow.

The molecule 4-Amino-5-phenyl-4H-1, 2, 4-triazole-3-thiol (APTT) has been studied as corrosion inhibitor by authors [7]. This molecule contain one co-ordinate ( $=N-$ ,  $-NH_2$ ) and one covalent ( $-S -H$ ) groups which can form a protecting film on the surface of mild steel through chemisorption. The aim of this reported work was focused on the turbulent flow effect on formation and stability of inhibitor (APTT) film. The influence of turbulent flow was investigated by changes in open circuit potential (OCP) with immersion time, potentiodynamic polarization, and electrochemical impedance spectroscopy (EIS) with a rotating cylinder electrode (RCE). To separate the effect of oxygen from the effect of rotation rate, experiments were conducted in oxygenated and de aerated solutions. The Molecular structure of APTT is shown as follows(scheme 1):



**Scheme 1.** Molecular structure of APTT

## 2. EXPERIMENTAL WORK

The working electrode employed in this work was made from mild steel, whose chemical composition is as follows: 0.08 wt.% C, 0.25 wt.% Si, 0.45 wt.% Mn, 0.03 wt.% P, 0.03 wt.% S, balanced with Fe. The rotating cylinder electrode (RCE) was designed for application with a Gamry Instruments Company, model AFMSRCEP rotator. The dimensions of the RCE were diameter 1.2 cm and length 0.8 cm. This produced a RCE active area of 3 cm<sup>2</sup>.

High-density polyethylene rod was used as an inert insulating sheath. The experiments were performed at different electrode rotation rates: 400 RPM ( $U_1= 25.12 \text{ cm s}^{-1}$ ), 800 RPM ( $U_2=50.24 \text{ cm s}^{-1}$ ), 1200 RPM ( $U_3=75.36 \text{ cm s}^{-1}$ ), 1600 RPM ( $U_4=100.48 \text{ cm s}^{-1}$ ) and 2000 RPM ( $U_5=125.6 \text{ cm s}^{-1}$ ) at 30°C. The selection of these ranges was based on the conditions commonly observed at industrial facilities.

The Reynolds number for a rotating cylinder electrode with outer diameter,  $d$  (cm) was calculated according to the relation [8]:

$$Re = \frac{U d \rho}{\mu} \quad (1)$$

where  $\rho$ ,  $\mu$  and  $U$  are the solution density ( $1.038 \text{ g cm}^{-3}$ ), the absolute viscosity of the solution ( $0.0102 \text{ g cm}^{-1} \text{ s}^{-1}$ ) and linear velocity ( $\text{cm s}^{-1}$ ). In general, for a rotating cylinder, when the Reynolds Number is greater than 200, then the flow is turbulent [9]. The calculated Reynolds number values ( $Re_1 = 3067.6$ ,  $Re_2 = 6135.2$ ,  $Re_3 = 9202.8$ ,  $Re_4 = 12270.4$  and  $Re_5 = 15338$ ) for the speed given above in which confirm that the experiments were performed under turbulent flow conditions. The working electrode was first mechanically polished using SiC paper in successive grades from 200 to 1500, washed with distilled water thoroughly and degreased with absolute ethanol and dried.

Experiments were carried out in oxygenated and de aerated 1.0 M HCl solutions, the electrode was immersed after the solution was purged with pure oxygen or nitrogen for 30 min and the solution was kept purged above the solution until the end of the experiment.

A Gamry water-jacketed glass cell of capacity 150 ml was used containing three compartments for working, graphite bar counter and reference electrodes. A Luggin-Haber capillary was also included in the design. The tip of the Luggin capillary is made very close to the surface of the working electrode to minimize IR drop. The reference electrode was a saturated calomel electrode (SCE).

The inhibitor was used through the experiments is 4-amino-5-phenyl-4H-1, 2, 4-triazole-3-thiol (APTT). According to our previous studies,  $4 \times 10^{-4} \text{ M}$  of inhibitor would be sufficient to obtain a good protective efficiency after 120 min. of immersion time in 1.0M HCl solution [7]. The solution was freshly prepared from analytical grade chemical reagents using distilled water and was used without further purification. For each run, a freshly prepared solution as well as a cleaned set of electrodes was used.

Electrochemical measurements were performed using Gamry Instrument Potentiostat/Galvanostat/ ZRA, these include Gamry framework system based on the REF 600, Gamry applications that include OCP, potentiodynamic scan and EIS are DC105 and EIS300 software. The potentiodynamic current-potential curves were swept from -0.2 to 0.2  $V_{\text{SCE}}$  at a scan rate of  $0.5 \text{ mV s}^{-1}$ . Impedance measurements were carried out using AC signals of amplitude 10 mV peak to peak at the open circuit potential in the frequency range 10 KHz to 0.1Hz. Before polarization and impedance experiments, the open circuit potential of the working electrode was measured as a function of immersion time during 120 min, the time necessary to reach a quasi-stationary value for the open circuit potential. All measurements were duplicated and only the average values were reported.

### 3. RESULT AND DISCUSSION

#### 3.1. Open circuit potential (OCP) with immersion time measurements

A corrosion potential evolution as function of time shows the best qualitative method for monitoring interface modification between a metal and its environment [9]. The OCP of mild steel was monitored over 120 min. from the moment of immersion in the test solution at  $30 \text{ }^\circ\text{C}$ . The effect of

different rotation rates on the variation of the OCP of mild steel with inhibitor in oxygenated and de aerated 1.0 M HCl solutions at 30 °C were conducted and the results is represented in Fig. 1. It was found that the OCP becomes more positive in oxygenated solution compared to de aerated solution. It means that the surface becomes nobler in presence of oxygen. Moreover, it's become nobler also with increased rotation rate due to more oxides formation on metal surface in high rotation rates. In fact increased presence of dissolved oxygen and H<sup>+</sup> ions on the surface of metal at higher rotation rates leads to formation of more oxides and more positive values of OCP. While in de aerated solution the surface become less noble with rotation rate which due to decrease in the rate of cathodic reaction that provided by the adsorption of APTT on cathodic site.

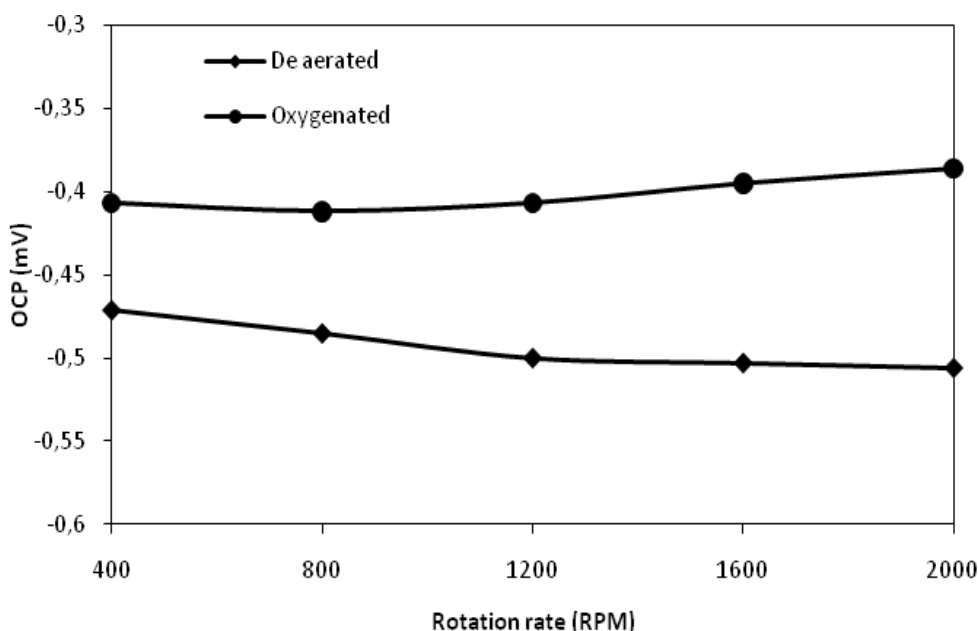


**Figure 1.** Open circuit potential vs. rotation rate for mild steel in oxygenated and de aerated 1.0 M HCl solutions with  $4 \times 10^{-4}$  M of APTT.

### 3.2. Polarizations

Potentiodynamic measurements were obtained for mild steel in oxygenated and de aerated 1.0M HCl solutions with and without  $4 \times 10^{-4}$ M of APTT at different rotation rates. In case of oxygenated solution, Fig.2, when the rotation rate increased the cathodic and anodic current densities are increased which due to an increase of the oxygen supply to the metal surface as well as it indicated an active dissolution of mild steel.

While in de aerated solution, Fig.3, the cathodic current densities were decreased and the effect of the increased rotation rate on the anodic dissolution of metal is low, this is due to the inhibitor formed film as flow can increase mass transport of inhibitor molecules that causes more inhibitor presence at metal surface [10].

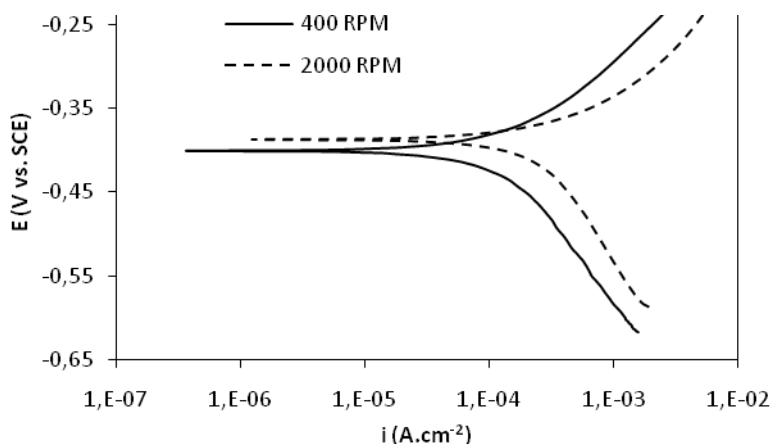


**Figure 2.** Polarization curves for mild steel in oxygenated 1.0M HCl solution with  $4 \times 10^{-4}$  M of APTT with 400 and 2000 RPM.

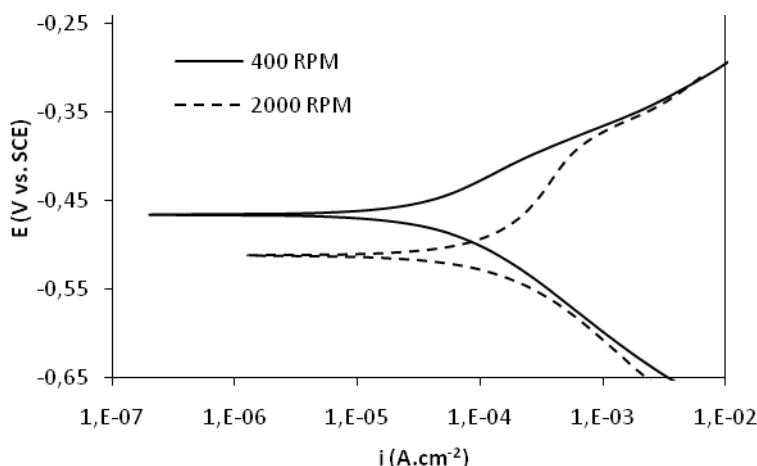


**Figure 3.** Polarization curves for mild steel in de aerated 1.0M HCl solution with  $4 \times 10^{-4}$  M of APTT with 400 and 2000 RPM

The polarization data, including corrosion current density ( $i_{corr}$ ), Tafel slopes ( $\beta_a$  and  $\beta_c$ ), and  $E_{corr}$ , for oxygenated and de aerated blank and inhibited solutions at 400, 800, 1200, 1600, and 2000 RPM are summarized in Table 1. The values of inhibition efficiencies ( $IE\%$ ) were also calculated using eq. [1] and depicted in Table 1 as follows:

$$IE\% = \frac{i_{uninhibit} - i_{inhibit}}{i_{uninhibit}} \times 100 \tag{2}$$

where  $i_{uninhibit}$  and  $i_{inhibit}$  are the corrosion current density without and with APTT, respectively

It was observed that at higher rotation rate the higher corrosion current densities, while  $E_{corr}$  followed the same trend of OCP measurement as mentioned in Section 3.1. Although the corrosion rate decreased with addition of APTT, the same trend decreases with increase in rotation rate in oxygenated solution in which indicating lower inhibitory action by APTT on the corrosion of the mild steel under given condition as it can be seen from IE% trend. IE% kept almost within narrow range of variation with rotation rate in de aerated solution. This trend may be attributed to the absence of oxygen effect.

**Table 1.** Polarization parameters for mild steel with and without  $4 \times 10^{-4}$  M APTT in oxygenated and de aerated 1.0 M HCl solutions at different rotation rates

Rotation speed (RPM)	$\beta_a$ (mV/ dec)	$\beta_c$ (mV/ dec)	$i_{corr}$ $\mu\text{A}/\text{cm}^2$	$E_{corr}$ mV	IE%
Oxygenated blank solution					
400	142	255	783	-383	
800	143	288	840	-371	
1200	159	311	1344	-367	
1600	211	345	1513	-358	
2000	225	358	1547	-353	
Oxygenated inhibited solution					
400	139	249	178	-400	77
800	175	345	274	-408	67
1200	227	323	500	-394	62
1600	238	319	597	-395	60
2000	294	320	639	-386	58
De aerated blank solution					
400	63.3	88.0	23.2	-443	
800	82.8	136.3	45.5	-436	
1200	62.5	95.6	55.9	-439	
1600	58.4	88.0	68	-443	
2000	72.8	93.4	78.7	-445	
De aerated inhibited solution					
400	71.8	93.1	13	-466	44
800	127.6	103.0	24.9	-473	45
1200	87.0	105.1	30.2	-498	46
1600	115.6	92.1	35.5	-503	47
2000	151.8	151.8	43.4	-512	44

It is generally accepted that the first step in the adsorption of an organic inhibitor on a metal surface usually involves replacement of one or more water molecules adsorbed at the metal surface [11]:



The inhibitor may then combine with freshly generated  $\text{Fe}^{2+}$  ions on steel surface, forming metal inhibitor complexes [32]:



The resulting complex, depending on its relative solubility, can either inhibit or catalyze further metal dissolution. It is insufficient to form a compact complex with the metal ions at low concentrations of APTT in the solution, so that the resulting adsorbed intermediate will be readily soluble in the acidic environment. But at relatively higher concentrations, more APTT molecules become available for complex formation, which subsequently diminishes the solubility of the surface layer, leading to improved inhibiting effect [12]. However, hydrodynamic conditions can also affect the inhibition of metal corrosion; flow can increase mass transport of inhibitor molecules that causes more inhibitor presence at metal surface. This effect can improve the inhibition performance [10]. Hydrodynamic conditions can increase mass transport of metal ions ( $\text{Fe}^{2+}$ ), produced during metal dissolution, from electrode surface to the bulk of solution and hence lead to less  $[\text{Fe-Inh}]^{2+}$  complex presence on electrode; this is a harmful effect for inhibition performance. In addition the high shear stress resulted from high flow velocity can also separate inhibitor layer or adsorbed  $[\text{Fe-Inh}]^{2+}$  complex and cause more desorption from metal surface which acts as a negative factor on inhibition efficiency [10].

### 3.3. EIS measurements

To quantify turbulent flow influence on film formation, EIS measurements were carried out at corrosion potential for five rotation rates after 120 min. of immersion time in oxygenated and de aerated 1.0M HCl solutions with and without  $4 \times 10^{-4}$  M of APTT. The magnitude of the impedance decreases from the beginning and up to the end of the experiments in both inhibited solutions, oxygenated and de aerated as shown in Nyquist plots, Fig.3 and Fig 4 respectively, It can be concluded from these figures that the impedance response of mild steel has significantly being changed with rotation rate. This can be attributed to the decrease of the substrate impedance with the increase of the rotation rate. The impedance spectra for mild steel for different rotation rate in oxygenated solution shows one depressed capacitive loop at low rotation rate, Fig.4a, while at high rotation rate shows different behavior, it is exhibit a straight line inclined at an angle of  $45^\circ$  to the resistive axis at high frequency, this is related to a diffusion phenomenon, and one capacitive loop at low frequency.

The impedance spectra in de aerated solution were shows that the Nyquist plot has one depressed capacitive loop, Fig.4b, which arises from the time constant of the electrical double layer, called constant phase element (CPE). Use of the CPE, defined by the values of  $Z_0$  and  $n$ , is employed

in the model to compensate for the inhomogeneities in the electrode surface as depicted by the depressed nature of the Nyquist semicircle [13]. CPE is defined in impedance representation as:

$$Z(\omega) = Z_0 \cdot (j \omega)^{-n} \tag{5}$$

where  $Z_0$  is the CPE constant,  $\omega$  is the angular frequency (in rad/s),  $j^2 = -1$  is the imaginary number and  $n$  is the CPE exponent.

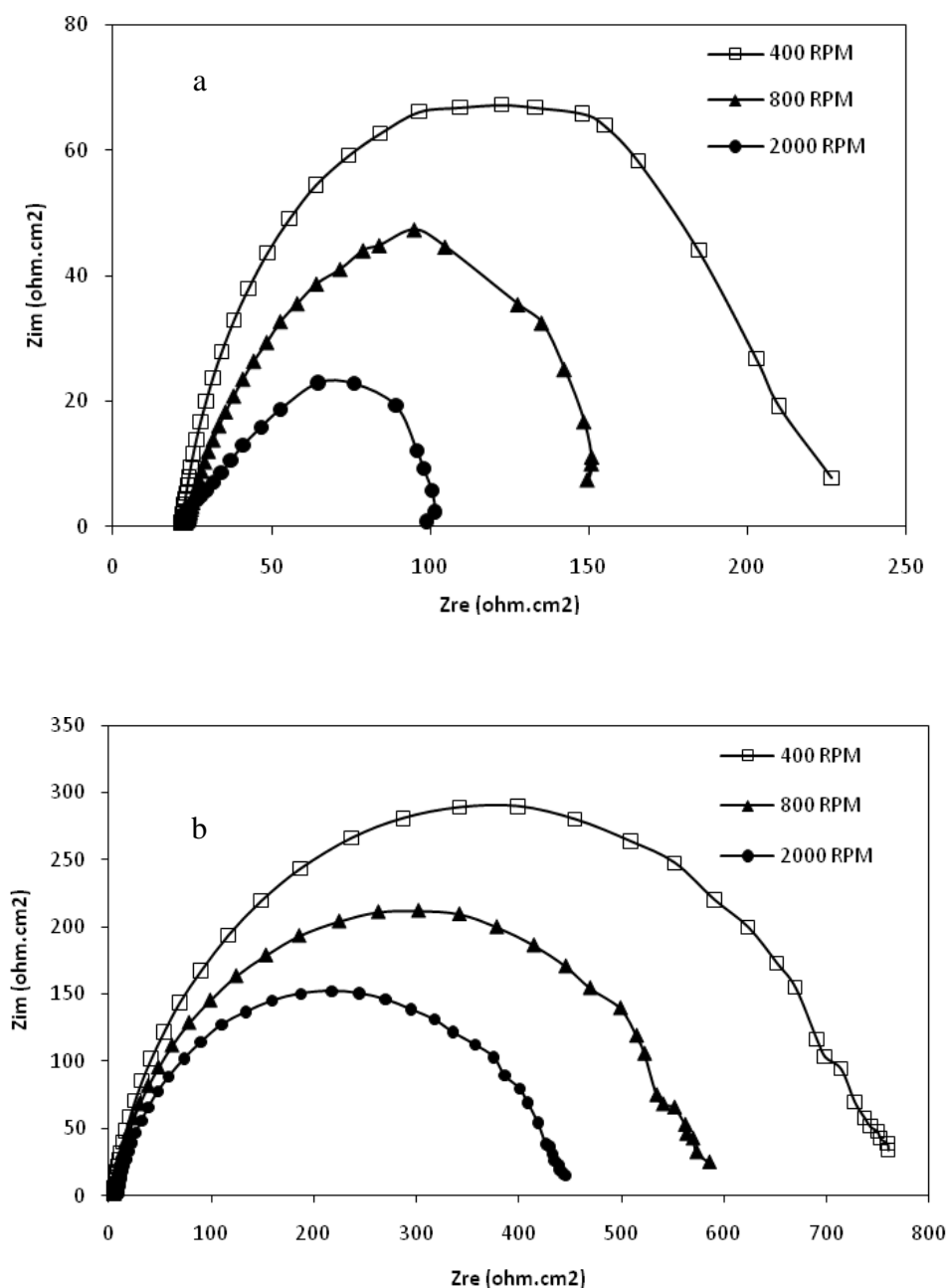


**Figure 3.** Nyquist plots for mild steel after 120min of immersion in oxygenated (a) and de aerated (b) 1.0M HCl solutions with  $4 \times 10^{-4}$  M of APTT at different rotation rates.

Evolutions of physical parameters concerning film and corrosion processes are discussed from an electric equivalent circuit (EEC), which models the interface, Fig 4. The circuit elements for data obtained for blank and inhibited for both oxygenated and de aerated solutions, include a solution resistance,  $R_s$ , a constant phase element, CPE, and a charge transfer resistance,  $R_{ct}$ . The value of  $R_{ct}$  is indicative of electron transfer across the interface. In the case of oxygenated solution at high rotation speed, equivalent circuit (Fig. 4a) should also have a Warburg impedance,  $W_\delta$ , in series with a  $R_{ct}$  because of straight line inclined at an angle of  $45^\circ$  at high frequency which is observed in the Nyquist diagrams. The values of circuit elements obtained for blank and inhibited for both solutions in different rotation rates are given in Table 2. The inhibition efficiencies, IE%, were also calculated using the following relationship:

$$IE\% = \frac{R_{ct\ inhibit} - R_{ct\ uninhibit}}{R_{ct\ inhibit}} \times 100$$

where  $R_{ct\ inhibit}$  and  $R_{ct\ uninhibit}$  are the polarization resistance with and without APTT.

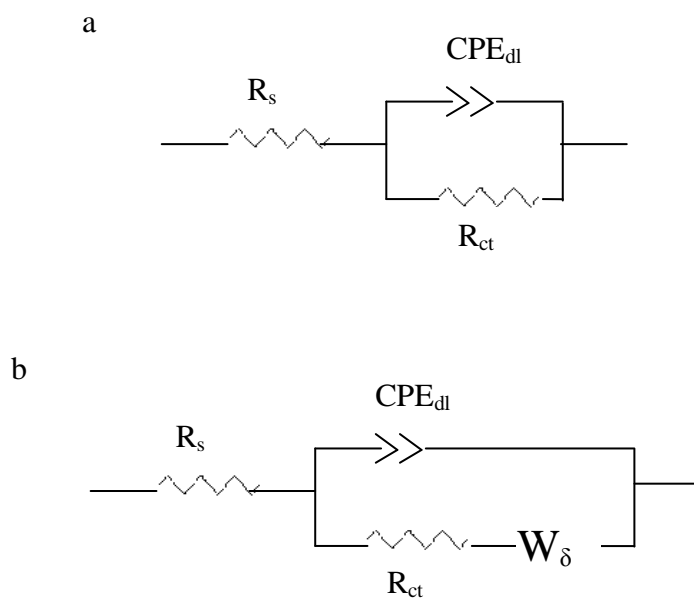


**Figure 4.** Equivalent circuit model used in the fitting of the impedance data of mild steel in oxygenated at low rotation rates and de aerated (blank and inhibited) solutions (a) and oxygenated (inhibited) solution at high rotation rate (b) .

Table 2 indicated that the charge-transfer resistances,  $R_{ct}$ , increase with the presence of APTT. A large charge-transfer resistance is associated with a slower corroding system [14]. In addition, a better protection provided by an inhibitor is associated with a decrease in capacitance of the metal [15].

The decrease in  $C_{dl}$ , which results from a decrease in local dielectric constant and/or an increase in the thickness of the electrical double layer, suggests that APTT acts via adsorption on the metal/solution interface [16].

With the increased rotation rate of the inhibiting HCl solution, the value of resistance  $R_{ct}$  significantly decreases, while the value of parameter  $C_{dl}$  increases. These results indicate weaker adsorption of the inhibitor on the electrode surface and lower protective properties of the surface adsorption layer. Inhibition efficiency in oxygenated solution was decreased with rotation rate which can be attributed to the increase of oxygen amount on the mild steel surface, while it kept almost constant in de aerated solution. The EIS results were found in line with those obtained by polarization method. The hydrodynamic factor had two opposite effects on inhibition performances. On the one hand, it increased mass transport of inhibitor molecules to the electrode surface which was beneficial to improving inhibition efficiency. On the other hand, high shear stress resulted from high flow velocity would also remove inhibitor films from metal surface which was harmful to inhibition efficiency [10].

**Table 2.** Impedance data for mild steel with and without  $4 \times 10^{-4}$  M APTT in oxygenated and de aerated 1.0 M HCl at different rotation rates

Rotation speed (RPM)	$R_s$ (ohm.cm <sup>2</sup> )	$R_{ct}$ (ohm.cm <sup>2</sup> )	$C_{dl}$ ( $\mu$ F. cm <sup>-2</sup> )	$n$	$W_\delta$	IE%
Oxygenated blank solution						
400	19.3	49.40	687	0.72		
800	21.2	36.37	782	0.68		
1200	37.41	37.33	841	0.68		
1600	31.23	25.60	915	0.65		
2000	28.11	26.13	967	0.58		
Oxygenated inhibited solution						
400	21.01	197.6	77.1	0.79		75
800	23.3	134.7	200	0.73		73
1200	58.36	109.8	200	0.68		66
1600	41.86	80	617	0.7	10,200	68
2000	37.7	67	781	0.64	28,580	61
De aerated blank solution						
400	10.7	341	61.6	0.9		
800	2.7	398	53.1	0.89		
1200	2.9	567	58.1	0.9		
1600	0.64	420	62.2	0.89		
2000	2.63	377	86.1	0.88		
De aerated inhibited solution						
400	4.34	730	29.3	0.88		43
800	4.52	561	29.9	0.85		45
1200	5.1	381	40.1	0.87		46
1600	3.94	460	38.7	0.83		47
2000	8.34	424	30.6	0.83		44

#### 4. CONCLUSION

The influence of turbulent flow on the corrosion inhibition of mild steel by APTT in 1.0M HCl solution was evaluated from OCP versus time, polarization curves and impedance data for different flow rates. Corrosion current density decreased with addition of APTT in solution, regardless the rotation rate. Inhibition efficiencies were found decreased with rotation rate in oxygenated solution; however it kept almost constant in de aerated solution.  $C_{dl}$  values were found decreased in presence of APTT but it increased proportionally with rotation rate. The formation and the development of the inhibitor film were dependent on the flow rate. Data from polarization and EIS shows that the inhibitor film showed a strong resistance against rotation rate in de aerated solution, but it straggling in oxygenated solution.

#### ACKNOWLEDGMENT

We gratefully acknowledge Universiti Kebangsaan Malaysia for support of this project under Grant no. UKM-GUP-BTT-07-25-170

#### References

1. P. Bommersbach, C. Alemany-Dumont, J. Millet and B. Normand, *Electrochim. Acta* 51(2006) 4011
2. D. Klenerman, J. Hodge and M. Joseph, *Corros. Sci.* 36(1994) 301.
3. J. Tan, S. Bailey and B. Kinsella, *Corros. Sci.* 38(1996) 1681.
4. J. Wharton, C. Barik, G. Kear, K. Wood, R. Stokes and F. Walsh, *Corros. Sci.* 47 (2005)3336.
5. N. Ochoa, F. Moran, N. Pebere and B. Tribollet. *Corros. Sci.* 47(2005)593.
6. J.L. Mora-Mendoza, J.G. Chacon-Nava, G. Zavala-Olivares, M.A. González-Núñez and S. Turgoose, *Corrosion* 58(2002)608
7. A.Y. Musa, A. A. H. Kadhum, M. S. Takriff, A. R. Daud, S. K. Kamarudin and N. Muhamad, *Corros. Eng., Sci. Tech.*, 45 (2010) 163.
8. R. Gabe, *J. Appl. Electroch.* 4 (1974): p. 91.
9. Technical note "Study of Mass-Transport Limited Corrosion Using Pine Rotated Cylinder Electrodes," Pine research instruments, LMECN200601, May 2006.
10. X. Jiang, Y. Zehang and W. Ke, *Corros. Sci.* 47 (2005) 2636.
11. J.O'M. Bockris and D.A.J. Swinkels, *J. Electrochem. Soc.* 111 (1964)736.
12. E.E. Oguzie and Y. Li, F.H.Wang, *J. Colloid Interface Sci.* 310 (2007)90.
13. H. Ashassi-Sorkhabi and E. Asghari, *Electrochim. Acta.*, 54(2008)162.
14. K.F. Khaled, *Electrochim. Acta* 48 (2003) 2493.
15. S. Hleli, A. Abdelghani and A. Tlili, *Sensors* 3 (2003)472.
16. K. Babic-Samardzija, K.F. Khaled and N. Hackerman, *Anti-Corros. Method. Mater.* 52 (2005) 11.